UNIVERSITY OF READING

Department of Meteorology

Baroclinic Weather Systems and Radiative Dust Feedback on Mars

Sarah Cleveland

A dissertation submitted in partial fulfilment of the requirement for the degree of MSc Atmosphere, Ocean and Climate

August 9th 2016

ABSTRACT

Of the atmospheres in our Solar System, Mars' is perhaps the most similar to Earth's. It behaves in many familiar ways, but significant differences in its circulation make it interesting to study. Dust is the main source of inter-annual variability on Mars, and its large regional and global dust storms are unique to its atmosphere. A low-order model describing the relationship between baroclinicity, heat flux and atmospheric dust constant has been adapted from Ambaum and Novak's non-linear oscillator model for the midlatitudes on Earth. The model was changed to be suitable for Mars, and the relationship of the dust to the other parameters was altered to produce realistic results. The question of whether the system shows an inherent chaos is discussed, and whether this chaos can be the main reason for interannual variability in dust storms.

CONTENTS

1

BACKGROUND

1.1 INTRODUCTION

While many of the planets and bodies in our Solar System are not rocky, nor have solid surfaces, out of those which do, only a few have atmospheres. There are a number of different atmospheres in our Solar System, but none so similar to our temperate, optically thin atmosphere as that of Mars. There is no wonder that humans have been fascinated by our celestial neighbour for hundreds of years - its potential for life, present or ancient, on its desert-like surface; its similar atmospheric temperatures which have recently been shown to allow small amounts of liquid water; decades of satellite missions, landers and rovers, as well as discussion of human exploration in the near future, have all captured the imagination of scientists and the general public alike.

Up close, however, while the Martian atmosphere seems to be the most similar to Earth's, it does exhibit notable differences. As can be seen in table 1, the atmosphere contains only about 1% of the mass of the Earth's, and is made up almost entirely of CO_2. Sunsets on Mars are blue, instead of red, due to an ever-present atmospheric dust content. More than a quarter of the mass of the air on the planet freezes into polar ice caps each winter, creating spiralling air patterns visible from space. Huge dust devils spin across the subtropics, and every few years, at seemingly random intervals, a dust storm engulfs the entire planet, blurring the surface in telescope images and compromising solar-powered probes and missions.

Parameter	Earth	Mars
Distance from Sun (km)	1.50 x 10^6	2.28 x 10^6
Distance from Sun (AU)	0.98 - 1.02	1.38 - 1.67
Mean Solar Constant, S_0 (Wm^{-2})	1367	589
Planet Radius (km)	6378	3396
Orbital Eccentricity	0.017	0.093
Planetary Obliquity	23.93°	25.19°
Rotation Rate, Ω ($10^{-5}s^{-1}$)	7.294	7.088
Length of Solar Day (seconds)	86,400	88,775
Length of Solar Day (hours)	23h 56m	24h 39m
Length of Year (Earth days)	365.25	687
Acceleration due to gravity at surface, g (ms^{-2})	9.81	3.72
Surface Atmospheric Pressure (Pa)	101,300	600
Surface Temperature (K)	230 - 315	140 - 300
Gas Constant, R (J kg^{-1} K^{-1})	287	192
Heat Capacity at constant pressure, C_p (J kg^{-1} K^{-1})	1003	850
Scale Height, H_p (km)	7.5	10.8
Dry Adiabatic Lapse Rate (K km^{-1})	9.8	4.5
Mean Buoyancy frequency, N ($10^{-2}s^{-1}$)	1.1	0.6
Deformation Radius, L (km)	1100	920

Table 1: Astronomical and meteorological parameters of Earth and Mars (adapted from Read and Lewis (2004)).

Earth	Mars
N_2 (77.09%)	CO_2 (95.97%)
O_2 (20.95%)	Ar (1.93%)
Ar (0.93%)	N_2 (1.89%)
CO_2 (0.04%)	O_2 (0.15%)

Table 2: Atmospheric constituents of Earth and Mars and their molar ratios (adapted from Read and Lewis (2004))

While the atmosphere acts somewhat differently to Earth's, it is familiar enough to meteorologists that Earth-based relationships and techniques can be modified for use in studying the Martian atmosphere. The Martian atmosphere plays host to baroclinic storms in the midlatitudes, which are well understood on Earth, and theoretical models can be altered slightly to account for Mars' smaller diameter, lower atmospheric density and smaller gravitational pull (see table 1). Dust is frequently lifted into storms - again, a familiar concept, as this is often seen on deserts on Earth. However, dust storms on Earth have never lasted months at a time and covered the entire surface of the planet, like those which occur on Mars every few years.

Figure 1 shows a series of images from NASA's Opportunity rover taken over 30 Martian days (sols) in 2005. This global dust storm blocked 99% of the incoming solar insolation to Opportunity and her sister rover, Spirit. Spirit never recovered from this storm, due to her solar-charged batteries losing power, and failing to provide enough warmth for the rover to function.

Water is a negligible factor in the lifecycle of baroclinic storms on Mars, although when the storms contain dust, the heating of the dust by the sun is important for the growth and development of storms of all types.

The motivation of this dissertation is to discover the nature of the dust within storms, and how it affects the growth rate and lifecycle of storms. Global dust storms only occur every two to three years, and this dissertation asks why large dust storms do not occur every year, and where this variability arises. It also aims to understand why the global dust storms are the most unpredictable aspect of the Martian climate, and if this unpredictability arises from any inherent chaos of the system.

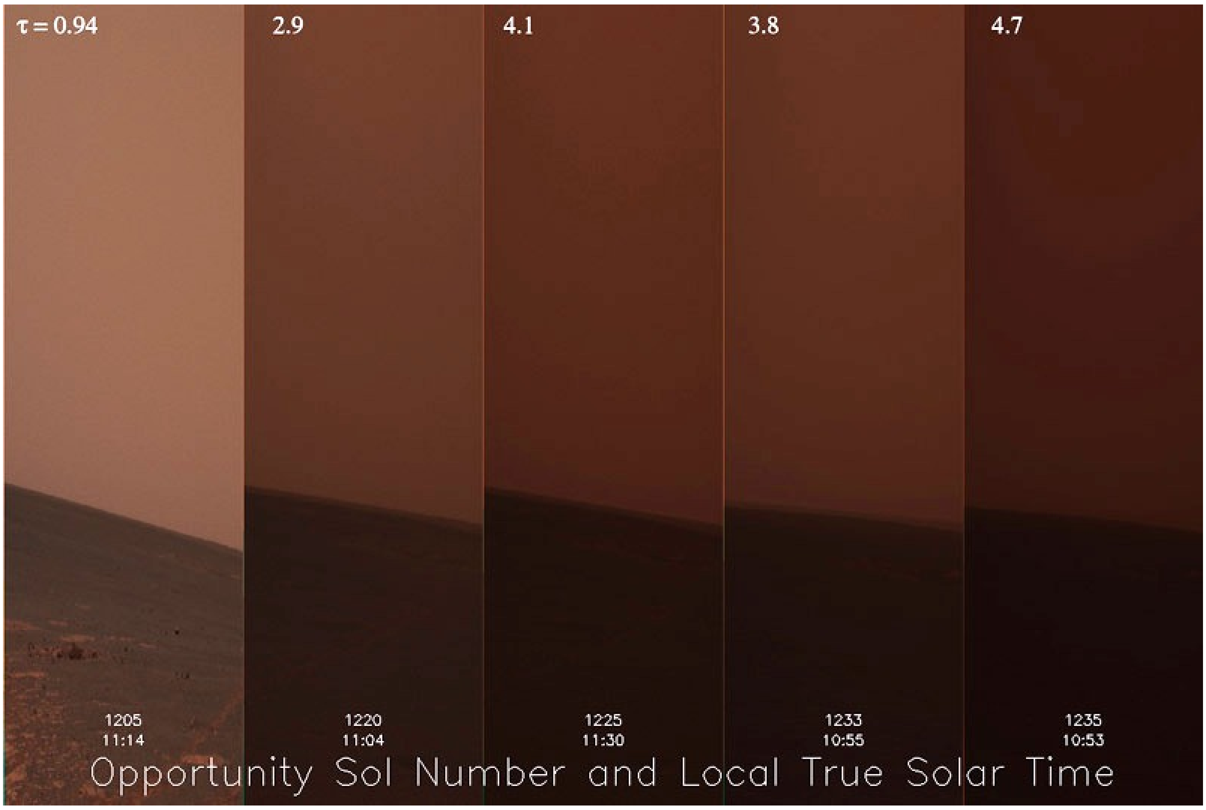

Figure 1: Images taken over the course of 30 sols by Opportunity rover of Mars' surface during the 2005 global dust storm event. The $\tau = 4.7$ image corresponds to 99% of solar insolation scattered or absorbed by dust. (MOC image MOC2 172 MSSS, courtesy of NASA/JPL and Malin Space Science Systems)

1.2 evidence of baroclinic instability on mars

From the early days of Martian exploration, it has been hypothesised that weather systems should exist on Mars. Flaugergues observed yellow clouds in 1809 (Read and Lewis (2004)) - now known to likely be dust-filled storms. Decades even before any satellites were put into Martian orbit, or landers on its surface, Hess (1950) predicted baroclinic eddies in Mars' winter hemisphere. Modern research, aided by numerous landers and dozens of satellites, has revealed coherent baroclinic eddy activity. Pictures from Mariner 9 show front-like cloud structures, and pressure data from surface measurements shows wave activity with a highly coherent structure (Collins et al., 2006). Similar photos can be seen in figure 2.

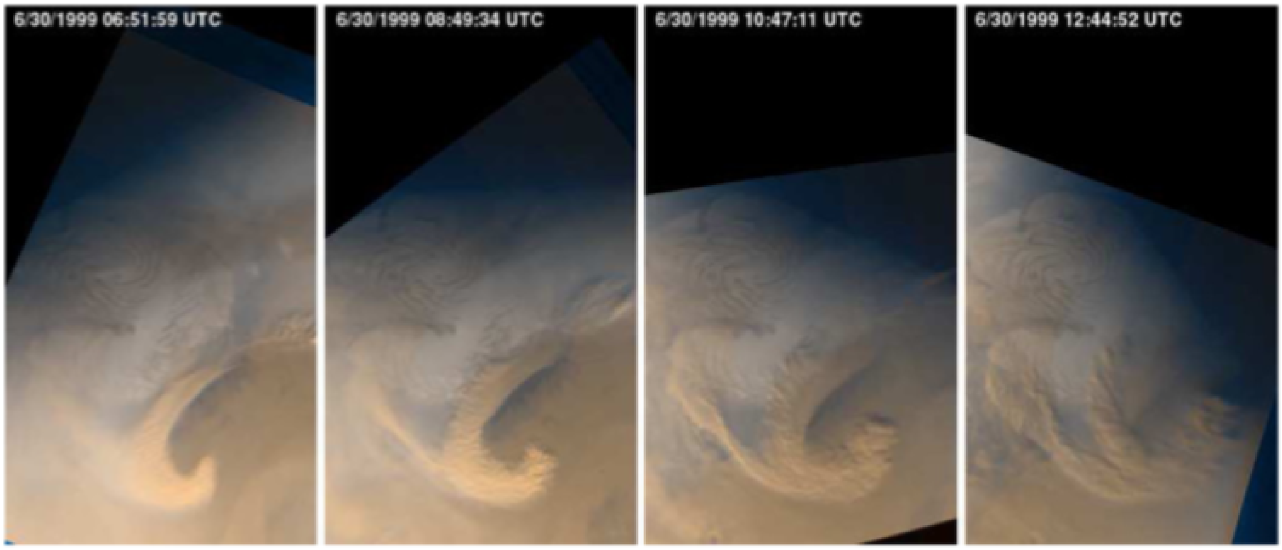

Figure 2: Images taken by the Mars Orbiter Camera (MOC) on board the Mars Global Surveyor of a baroclinic dust storm, photographed in June 1999. Dust clouds make frontal structures visible from space and from Earth. (MOC image MOC2 172 MSSS, courtesy of NASA/JPL and Malin Space Science Systems, via Read et al. (2015))

Baroclinic activity occurs exclusively in the Martian mid-latitudes, as is the case on Earth. Storms are significantly more likely to occur in winter than in summer, and - due to differences in topography (see figure 3) and placement of orbit - instability is stronger in the northern hemisphere winter than the southern hemisphere winter.

1.3 DUST ON MARS

Mars has negligible liquid water - certainly, not enough to significantly impact the global circulation or large-scale weather systems. A lack of moisture, oceans and change in atmospheric albedo from clouds would imply a simple structure of the Martian atmospheric circulation.

However, the effect of dust cannot be ignored. Dust is the main feedback mechanism on Mars which adds an aspect of unpredictability and, potentially, chaos to the atmosphere. Large-scale dust storm activity is probably the main source of inter-annual variability in

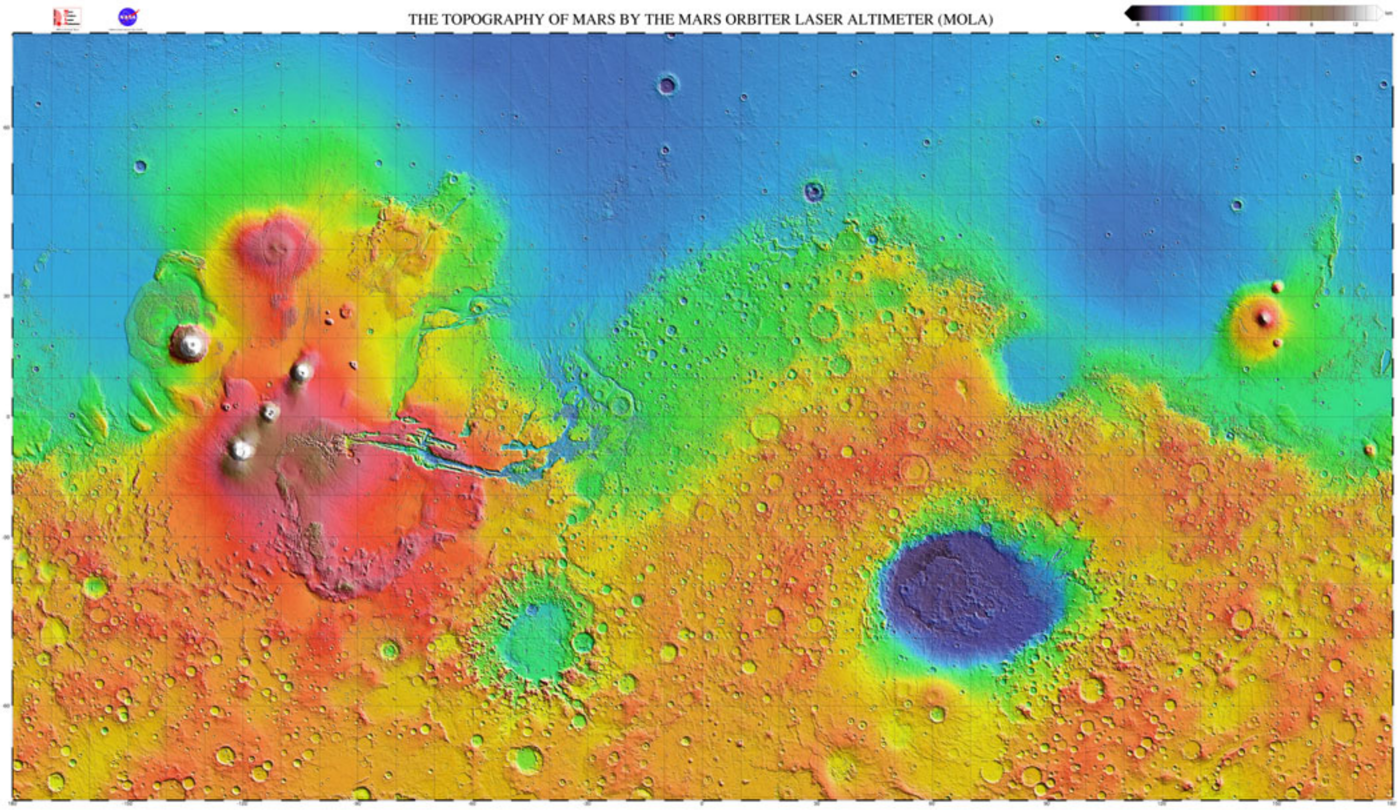

Figure 3: Topography map of Mars, showing the so-called 'hemispheric dichotomy'. The mean altitude of the southern hemisphere is several kilometers higher than the northern, making it more baroclinically stable. The poleward downhill slope in the northern hemisphere is thought to enhance the baroclinicity, according to Blumsack and Gierasch (1972). (Images from Mars Orbiter Laser Altimeter (MOLA), taken from http://mola.gsfc.nasa.gov/images.html (accessed 2016))

the Martian atmosphere, due to its non-linear relationship to the general circulation, and the complex feedback mechanisms dust has with surface winds and the heating of the surrounding air.

Dust uplift, transportation and distribution can strongly affect the global circulation and weather patterns on short- and long-scales, but is very difficult to predict. Even if Martian atmospheric measurements were made as densely as those on Earth (as it is, there are only around half a dozen working points of surface measurement over the whole planet), the dust uplift and deposition happens on very small scales which can cause a big impact. Mars is, in essence, a global desert, so analogues on Earth can be studied to gain a fair idea of the behaviour of Martian dust.

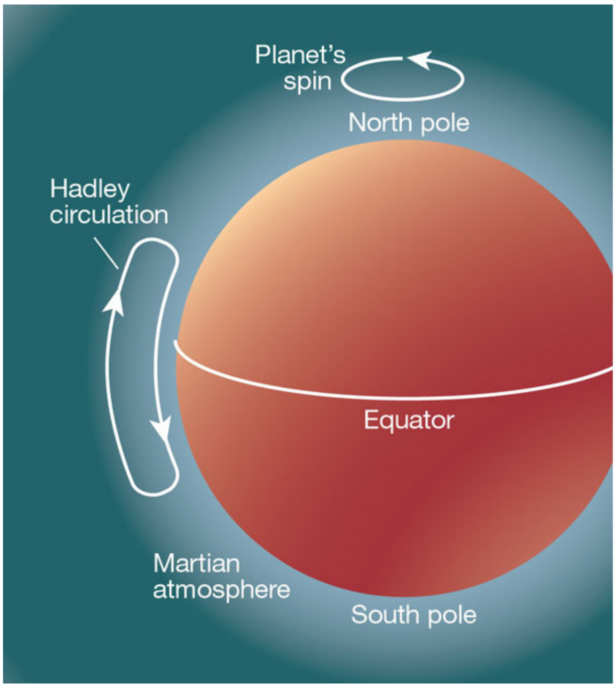

Figure 4: Global circulation of Mars, showing the cross-equatorial Hadley cell (from Gierasch (2002)

Dust can be considered to be a kind of analogue of the effect of moisture in a storm, as its heating effect on the surrounding air can be similar to the effect of latent heat release from condensation. It is a weak analogue, but the basic behaviour is a starting point for considering the heating effect of dust in a storm. This heating has various effects on different types of circulation. In a dust devil (see next section for a detailed description of the nature and structure of dust devils), addition of dust causes extra heating, which enhances the height and strength of the devil (Fuerstenau 2006). In the Hadley Cell (see figure 4), dust acts to enhance the winds and increase the meridional extent of the cell (Read and Lewis, 2004).

In a baroclinic storm, it is anticipated that addition of dust will enhance the winds and strength here, too, though there are competing effects. For example, an area blanketed by a large amount of atmospheric dust, such as in a global dust storm, experiences a reduction in wind speed and eventual dust settling. This is due to the sun only being able to heat the upper levels of an optically thick dust layer, which creates a temperature inversion and increases the static stability.

This suggests that addition of dust will first act to enhance wind speeds and strengthen circulations, up until a certain point, where dust eventually weakens the circulation and settles. It is the effect of this non-linear relationship that this dissertation aims to explore.

1.4 DUST DEVILS

Dust devils occur frequently on Earth, so have been well studied in desert regions, especially by Sinclair (1973). They can be anywhere from a few meters to more than 100m in diameter, and reach to the top of the convective boundary layer. Dust devils do not necessarily contain dust, but it is the dust which makes them visible, so more devils are recorded which contain dust than those which do not. Dust devils must not be confused with tornadoes, which have similar circulations but occur in different situations - the circulation of tornadoes arises from maintaining geostrophic balance, where dust devils maintain cyclostrophic balance, and thus can rotate either clockwise or anti-clockwise. Dust devils usually occur on clear days, on flat plains, when the heating from the sun is at its strongest in early summer afternoons.

Such is also the situation on Mars - the peak time for dust devils to occur is in southern hemisphere summer, on the large plains in the subtropics. This coincides with Mars' perihelion, and it is hypothesised that this timing is important for the onset of global dust storms. Dust devils can also be much larger on Mars, reaching up to several hundred metres across, and their shadows and tracks are often visible from orbiting telescopes.

Dust devils are of particular interest to this dissertation, as they are one of the main mechanisms for uplift of dust into the Martian atmosphere, as will be explained in the next section.

Consider two parcels of air, dense with dust, inside dust devils on Earth and on Mars. The equation

$$\rho dq \sim \rho c_p dT \tag{1}$$

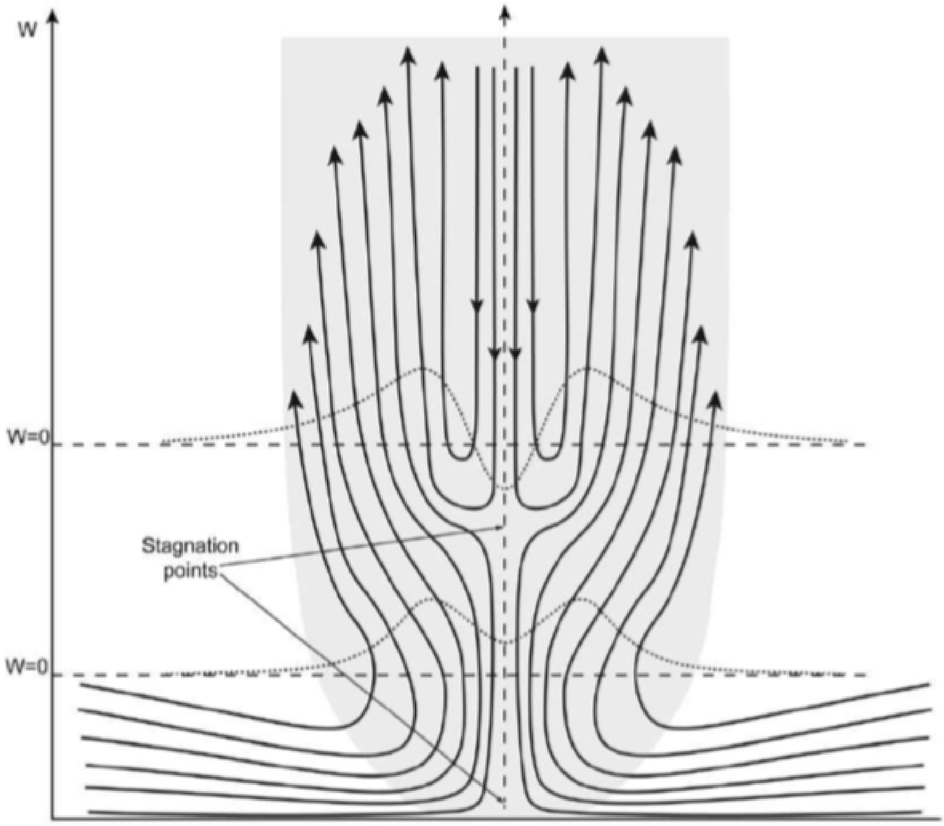

Figure 5: Possible flow inside a dust devil, from Balme and Greely (2006). Solid lines - radial and vertical flow directions; dotted lines - vertical wind speed profile at that height.

describes the rate of heating, where ρ is the air density, which around 100 times smaller on Mars, and where c_p has a smaller value on Mars than on Earth (see table 1). If the parcels receive the same amount of solar radiation, the heating of the dust per unit volume would be approximately the same, but due to Mars' less dense atmosphere, there would be a change in temperature in the Martian dust devil which is about 100 times as much as that on Earth.

For this reason, dust devils play a more dominant role in Martian circulation than in Earth's. The convective boundary layer is also higher on Mars, and Martian dust devils can stretch nearly ten times as high as those on Earth - about 8km - and hence dust can be injected more deeply into the atmosphere (Read and Lewis, 2004).

1.5 dust uplift on mars

One of the most important measures to understand, if one wants to understand dust's role in the Martian circulation, is how much dust is picked up and is allowed to circulate in the atmosphere, and what relationship this has to wind speeds or frequency of storms. From Newman et al. (2002a), two main mechanisms for dust uplift are identified - saltation and dust devils.

Dust particles on Mars are, on average, smaller than typical desert dust on Earth. The average size of particles suspended in the Martian atmosphere is 1-2μm, and for particles of this smaller size, inter-particle cohesion due to van der Waals forces act to inhibit uplift. Considering these factors, the calculated threshold wind speed required to lift dust particles of this size into the atmosphere are of the order of several hundred ms^{-1}, which are extremely improbable wind speeds for the Martian surface (Newman et al. (2002a)).

For this reason, there must be another mechanism which lifts the small particles into the atmosphere. Newman et al. (2002a) put forward that lifting and rapid saltation of sand and bigger particles (see figure 6) reduces the threshold speed required, as saltation effectively increases the surface stress, and increased surface stress increases the effective 'drag velocity' of the wind, which are related by:

$$u_{drag} = \sqrt{\frac{\zeta}{\rho}} \quad ms^{-1} \tag{2}$$

where ζ is an effective surface stress, which includes the effects of surface winds and sand impacting the ground during saltation, and ρ is the density of the surrounding air.

Therefore, the reduction in threshold velocity reaches reasonable levels, and depends on particle diameter D_p, the particle mass density of the dust ρ_d (which can be 5 orders of magnitude higher than surrounding dust density) and an unknown coefficient A:

$$u^t_{drag} = A\sqrt{gD_p\frac{\rho_d - \rho}{\rho}} \quad ms^{-1} \tag{3}$$

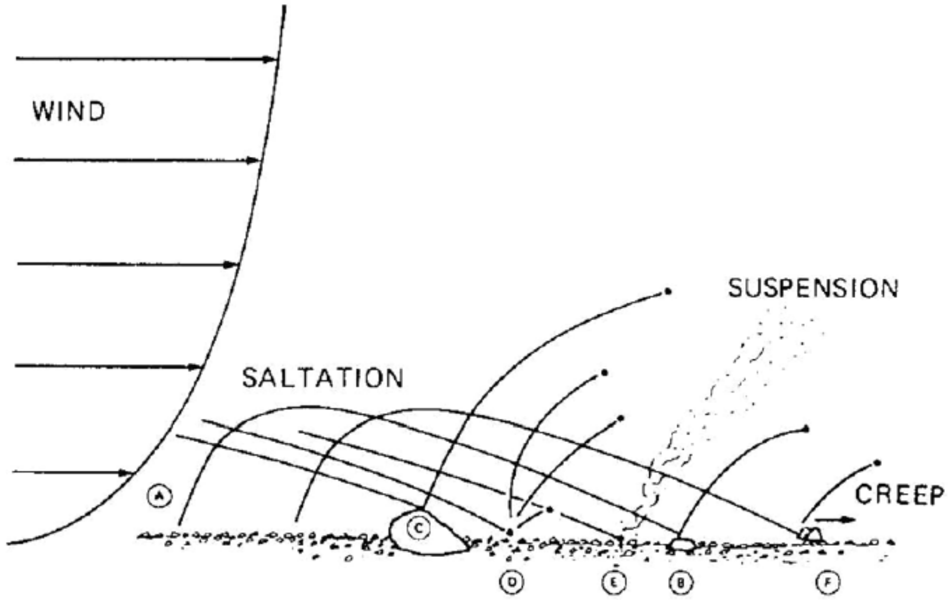

Figure 6: The process of saltation (after Greely and Iverson (1985)). Small particles become more easily suspended by this process; quickly saltating sand increases surface stress and picks up smaller particles.

Once this threshold is reached, the horizontal flux of sand particles (which is considered to be proportional to the vertical flux of dust particles as $V_D = \alpha_D H$, due to the effect of the saltation) is related to the drag velocity by:

$$H(u_{drag}) = 2.61\frac{\rho}{g}(u_{drag})^3(1 - \frac{u^t_{drag}}{u_{drag}})(1 + \frac{u^t_{drag}}{u_{drag}})^2 \quad kgm^2s^{-1} \tag{4}$$

Which for our purposes can be simplified to:

$$\text{Vertical flux of dust particles} \propto (u_{drag})^3$$

if $u_{drag} > u^t_{drag}$.

The other main mechanism for dust uplift into the Martian atmosphere is dust devils, as explained previously (Newman et al. (2002a)). Dust devils lift dust through vortical suction, the strength of which is related to the tangential wind speeds near the bottom of the dust devil. To find the vertical flux of dust in this situation, one can consider the tangential velocity required to lift n layers of dust, considering a layer to be one particle thick:

$$v_{tang} = (1 + \frac{15}{\rho_d g n D_p})^{\frac{1}{2}} (\frac{\rho_d g n D_p}{\rho})^{\frac{1}{2}} \quad ms^{-1} \tag{5}$$

where ρ_d is the mass density of dust particles, g is the gravitational constant, D_p is the average diameter of dust particles, and ρ is the density of the surrounding air. Greeley and Iversen (1985) simulated dust devils in the lab, so the tangential velocity was empirically found to be related to the vertical flux by:

$$V_D = \alpha_N (\frac{\rho v_{tang}^2 - 15}{g}) \quad kgm^2 s^{-1} \tag{6}$$

where α_N is another unknown constant.

Simplified for our purposes to:

$$\text{Vertical flux of dust particles} \propto (v_{tang})^2$$

if $\rho v_{tang}^2 > 15 kgm^{-1} s^{-2}$.

The coefficients A, α_N and α_D are dependent on the size of the particles and must be determined empirically. For the purposes of this paper, these coefficients do not need to be known, and it is only the relationships of the dust flux to the surface wind speeds which is of importance. It may also be assumed that the threshold velocities are frequently reached and exceeded on the Martian surface. Considering the amount of dust which the Martian atmosphere is frequently seen to hold, this is probably the case, and dust is picked up quite easily by reasonable surface wind speeds.

It is not known which method is more important for dust uplift, or what proportion of dust either method contributes to the total atmospheric dust. This may vary from year to year, and will depend on 'gustiness' and dust devil frequency, which in turn depends on the surface sensible heat flux. It is also difficult to measure, due to the relative lack of surface and satellite observations for Mars. The contribution to the total dust in the atmosphere by either method is unknown, so it is assumed that both methods contribute to dust uplift in similar magnitudes.

1.6 heating by dust

As mentioned previously, heating by dust can be considered to be somewhat analogous to latent heat released by moisture in storms on Earth. This heating acts to enhance dust devils, storms and the Hadley cell. An analysis by Fuerstenau (2006) used a photo of a dust devil taken by the Mars Orbiter Camera to determine the proportion of solar insolation absorbed by the dust devil itself. They determined that the proportion of absorbed sunlight by dust was 11%.

The approximate cross-sectional area of dust in 1 cubic meter of Martian air is 0.012 m^2, found by multiplying the cross sectional area of a 3μm particle ($7x10^{-12}m^2$) by the number of particles in a cubic meter ($1.7x10^9$, which is found by considering the mass density of dust, which can be 4 orders of magnitude higher than the level of dust in a clear atmosphere, at $7x10^{-5}$kg m^{-3}). Thus, considering 430W/m^2 of late afternoon Martian solar irradiance, 5.2W comes into contact with dust in a cubic meter. If 11% of this energy is converted into heat and quickly transferred to the surrounding air to maintain thermal equilibrium, 0.57W of energy acts on the air, which, consisting largely of CO_2, has a heat capacity of about 860 J/kg/K. Using values from table 1, it can be calculated that 0.57W of energy will raise the temperature of the air by 0.051°C per second.

A temperature rise of this rate causes convective instability in the area. A sufficiently large updraft should even cause the heated parcel within the dust devil to take on a super-adiabatic lapse rate. Fuerstenau cites this excess buoyancy as the reason for Mars' dust devils being much larger and prominent than on Earth.

The key questions in response to this are to determine how the location of the dust in a dust devil or storm affects its heating rate and life cycle. Dust heating is different from latent heating because of one important factor - unlike moisture, dust does not condense out of the system as pressure decreases. The heating of the dust with height at low concentrations may be approximately constant: the sun will preferentially heat dust which is higher in the atmosphere, but the amount of dust that can be held by the air decreases exponentially with height, like atmospheric pressure.

1.7 CHAOS AND NON-LINEARITY IN THE MARTIAN ATMOSPHERE

The nature of atmospheric motion is inherently sensitively dependent on initial conditions, and can exhibit so-called 'chaotic' behaviour, as shown by Edward Lorenz in 1963. The atmosphere of Mars is no exception, although unlike on Earth, where chaos theory manifests as an inherent limit of predictability of atmospheric motion, Martian atmospheric motion appears to be more regular and predictable than that of Earth's (Read and Lewis, 2004). Martian probes have recorded pressure patterns that seem to have a high amount of regularity for periods longer than a month, which would be more than double the theoretical limit of predictability for Earth.

Yet, on the longer time scales, the inter-annual circulation on Mars seems to contain at least as much variability as on Earth - the year in which a global dust storm is going to occur is hard to predict, except that it is very likely not to occur in two consecutive years.

Ingersoll and Lyons (1993) analysed the nature of these global dust storms, addressing why they do not occur every year. They used the relationship of the dust distribution and the Hadley circulation in a model which used the forcing by the seasonal cycle to determine how the atmospheric dust content affected the circulation in subsequent years. They found that one of their models produced periodic effects, and the other produced aperiodic, or chaotic results.

Thus it is possible that an element of chaos is influencing the long-timescale behaviour of the Martian atmosphere - certainly it is clear from previous sections that when one considers the relationship of dust with the atmosphere, it is very complex and non-linear. The Poincaré-Bendixson theorem states that if a system is described by three or more differential equations, it has the potential to show chaotic behaviour. The model used in this dissertation considers a simple two-parameter circulation oscillator, but adds a third parameter: dust.

2

METHOD

2.1 NUMERICAL MODEL

In order to solve the differential equations required for the problems in this project, a model was developed in python. It was required to have the ability to solve any given number of ODEs for any system. A simple forward-Euler method is unsuitable for solving systems which may contain chaos, as the method has inherent drifting behaviour which will erase the natural non-self-repeating behaviour of a chaotic system.

The method chosen is a 4th order accurate Runge-Kutta solver. This a stable and accurate method, and the code was written such that any set of differential equations can be solved, and any number can be solved together - the model works equally well for sets of 2 or 3 equations, and any number of constants and parameters.

Below in figure 7 is the model's output for Lorenz's famous butterfly attractor (Lorenz, 1963), which was run as a test of the model's ability.

2.2 BUILDING THE EQUATIONS

The equations for this project were developed on a basis of Ambaum and Novak's (2014) non-linear oscillator equations describing the predator-prey feedback mechanism between baroclinicity in the mid-latitudes and eddy activity on Earth. The equations describe a

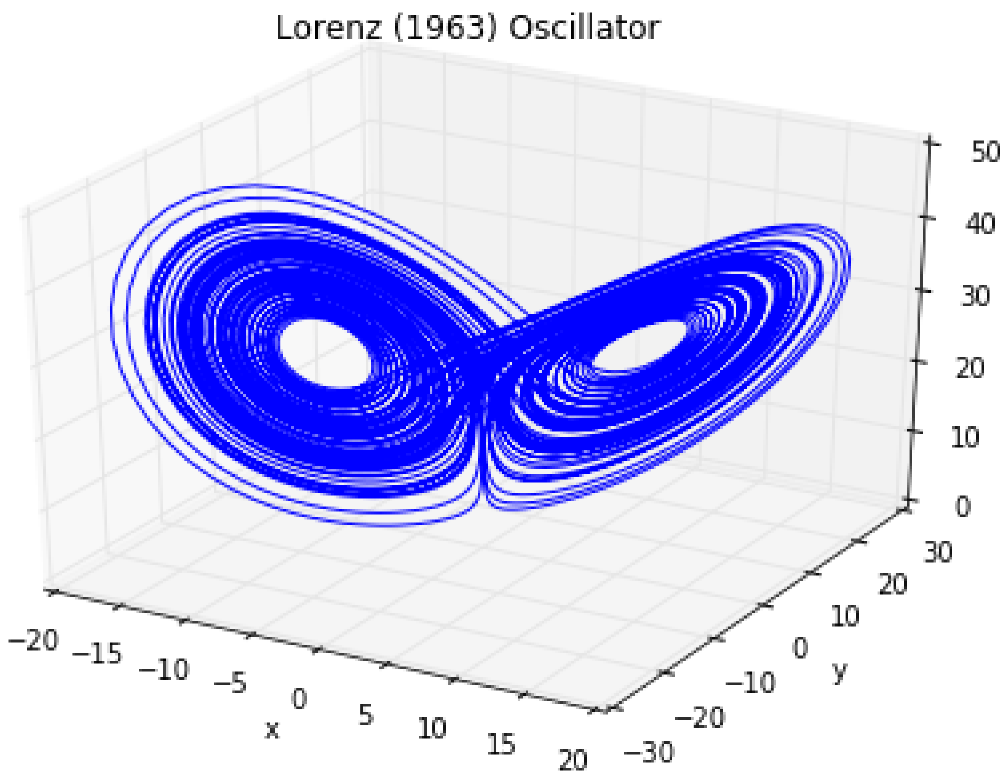

Figure 7: A phase space diagram of Lorenz's atmospheric convection model.

simplified system in which the baroclinicity in the mid-latitudes causes eddies to form, and these eddies eventually cause the baroclinicity to decrease and thus destroy the eddies.

Ambaum and Novak's equations are:

$$\dot{s} = F - f \tag{7}$$

$$\dot{f} = f(s - s_0) \tag{8}$$

where f is representative of the baroclinicity, s is representative of the heat flux, F is the forcing of the mean wind by radiation, and s_0 is the linear damping of eddies.

Figure 8 shows the model's output for Ambaum and Novak's equations. You can clearly see the relationship of the feedback in this highly regular function.

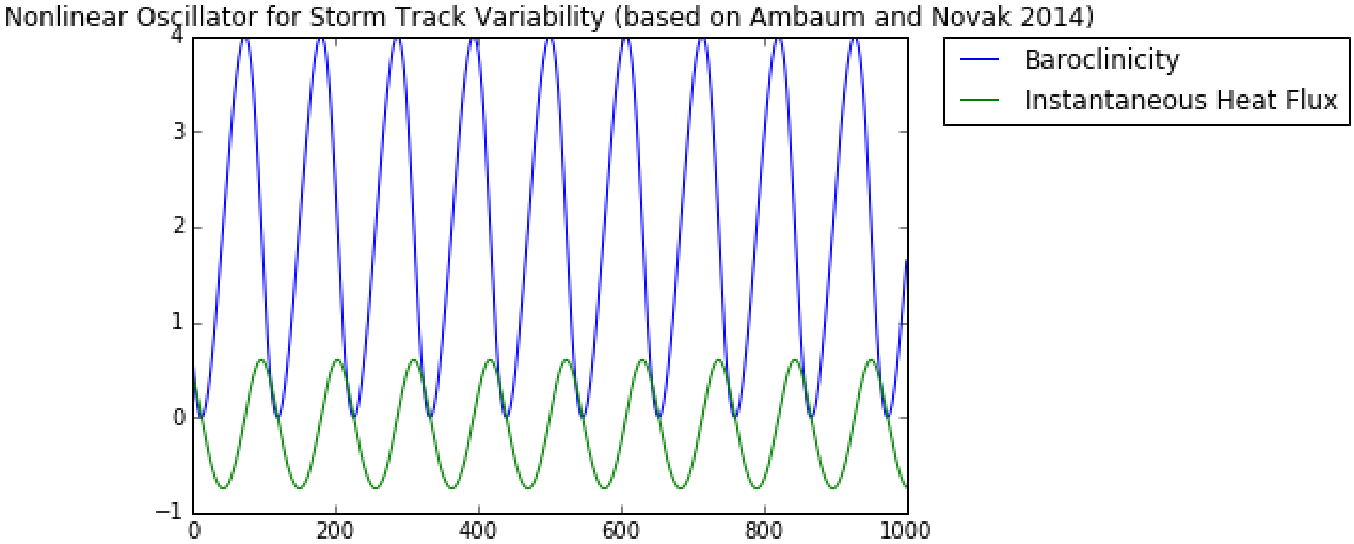

Figure 8: Ambaum and Novak's function describing the relationship between baroclinicity and instantaneous heat flux in the storm zones in Earth's midlatitudes.

This same behaviour is exhibited in a system with two species of animals: prey and its predator. If the population of the prey increases, the predator eats well and breeds profoundly the following year. The excess of predators causes the prey to die out much more quickly, and thus the predator has lost its food source and its population reduces in the following season. With the reduction of predators, the prey has a population boom. Figure 9 is a representation of Canadian lynx and mink populations based on the Hudson Bay Company's fur hunting figures. You can see that the populations are closely linked and the predator population follows the prey population on a slight delay. If a third species were to be introduced into the system, with a relationship to one or both of the earlier species, a very complicated system would form. This would potentially introduce chaotic behaviour.

2.3 ADDING PASSIVE DUST

To solve the questions asked by this dissertation, and in the context of Mars, a third parameter was added - the relationship of atmospheric dust concentration to the other variables. It has been mentioned previously that stronger wind speeds pick up more dust,

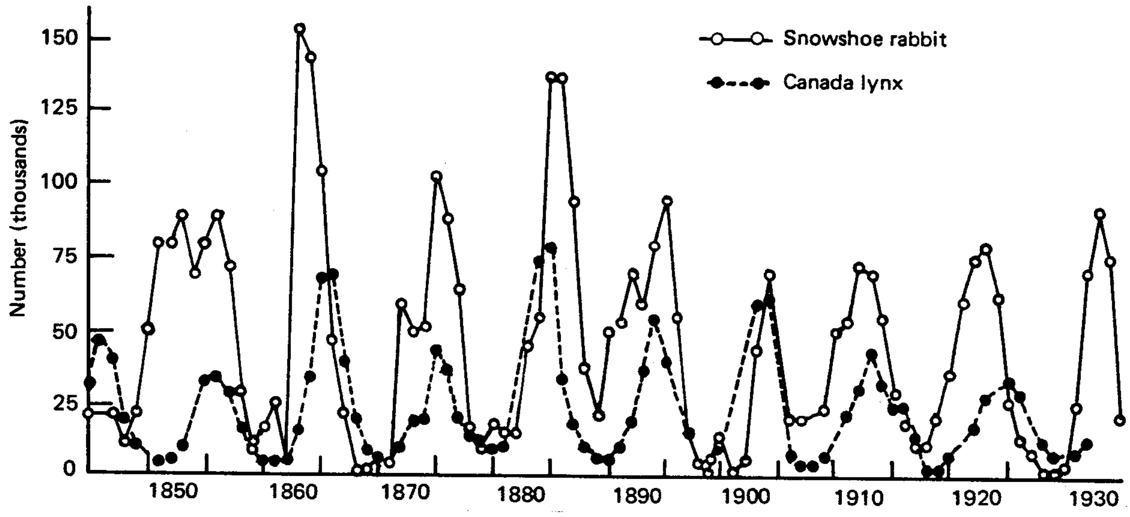

Figure 9: A proxy for Canadian Lynx and Snowshoe hare populations based on fur trading figures of the Hudson Bay Company. This predator-prey feedback can be seen in many aspects of nature, beyond just the literal sense. (via Verhulst (1985))

but at some point, the amount of dust in the atmosphere causes the winds to reduce. It is clear therefore that the dust concentration and the wind speeds/baroclinicity have a non-linear relationship, but it is not known whether it is realistic for the dust concentration to also have a direct relationship to the heat flux.

Initially, Ambaum and Novak's original equations were kept as they were, with a third equation added to describe the nature of the atmospheric dust content. The dust content was allowed to be altered by the baroclinicity and the heat flux, but the dust was not allowed to alter these variables yet. This is known as 'passive' dust, as it does not affect the other parameters, radiatively or otherwise. Of course, we know this is unrealistic and will produce periodic, non-chaotic behaviour. It is interesting to investigate nonetheless, and allows the dust uplift and deposition parameters to be tuned.

Further to this, the constants of the system were changed. Initially, the forcing of the mean wind was left as a simple constant value, but for the next test, an annual forcing cycle was introduced, which was a simple sinusoidal function. The seasonal cycle on Mars, however, is uneven, due to the eccentricity of the orbit. It is much greater (0.093) than that of Earth's (0.017), so southern hemisphere summer is significantly warmer than that of the northern hemisphere. Therefore a weighted sinusoidal function would be perhaps even more realistic. Furthermore, it is known that the heating of the Martian surface is altered when there is a lot of dust present in the atmosphere, so it would perhaps to be even more realistic to include this factor in the forcing parameter.

It is worth noting that in the summer hemisphere, the region which receives the most sunlight is the pole. On Earth, this makes little difference to the baroclinicity due to the hysteresis of the atmosphere, and the equator-pole albedo gradient, which remains throughout the summer. However, on Mars, where there are no oceans and little moisture, the atmosphere responds rapidly to different levels of heating, and the hottest place on the surface in midsummer is the pole (see figure 10). This destroys the equator-pole temperature gradient which feeds the baroclinic storms, and, in fact, reverses it. Thus, a realistic scenario is to not only let the seasonal temperature gradient reduce to low levels or to zero, but to let it be negative, at least for a short time around midsummer.

It is also worth noting that, for the same reasons, daily temperature fluctuations on Mars have a much larger range than those on Earth, and temperatures change rapidly in response to sunlight. This can be so strong as to set up an m=1 standing wave, forced by the diurnal temperature variations, and this could be another important forcing mechanism. Read and Lewis (2004) suggested that this daily temperature variation could be considered a kind of vibration, which can occasionally 'kick' the system into one of two baroclinic modes. An oscillation on the order of a day may be worth including in the model due to its strong forcing properties, though it may be difficult to implement and may only produce a subtle alteration to the results.

Thus, to add a Martian seasonal cycle, the form of F in the Ambaum-Novak equations above was chosen to be:

$$F = p + (1 - p)\frac{cos(2\pi t)}{T} \tag{9}$$

where p was taken to be 0.4 and T was set at 100 units. This means that 100 time units in the model represents one Martian year, or 687 sols. As such, the time axis can be rescaled by a factor of 6.87 so the scale is in sols. There was also included a weak damping term for s, which helped to maintain the stability for a longer period of time. In this setup, the

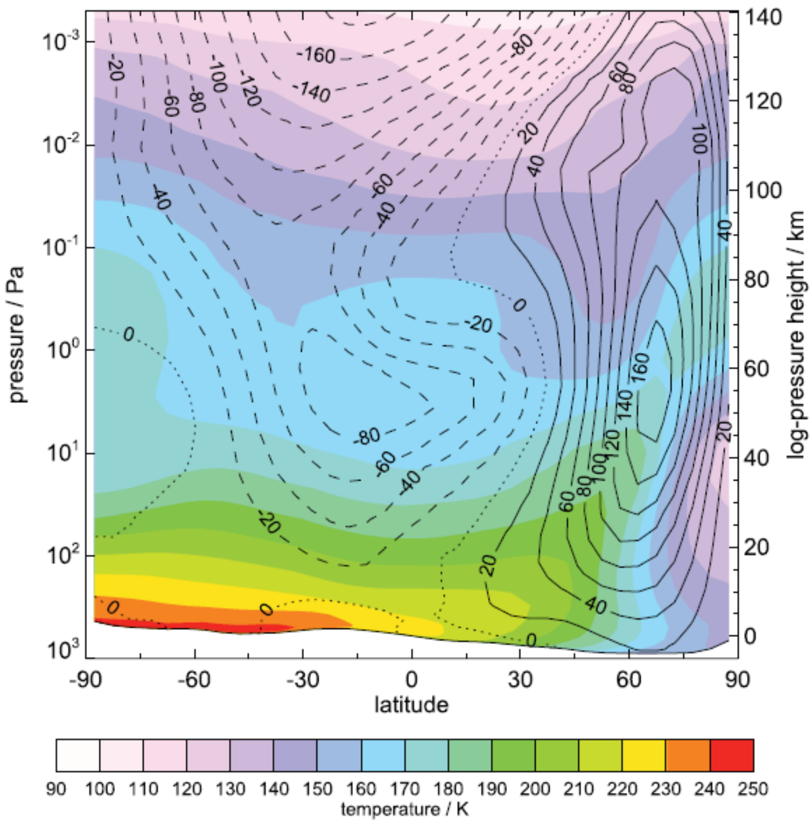

Figure 10: A map of temperature with height and latitude for the Martian southern hemisphere summer, near the solstice. The obliquity of Mars' rotation is around 25.1°, so the subsolar point here is at around 25 degrees south. This is also close to the point in the Martian year where it is closest to the sun, so these are some of the hottest temperatures seen in the Martian atmosphere. The contour lines also highlight the strong northern hemisphere winter jet.

mean wind is allowed to reverse during the summer, while maintaining a strong positive forcing through winter.

3

RESULTS

3.1 PASSIVE DUST

The basic form for the third equation describing dust was:

$$\dot{d} = \alpha(f^2 + s^2) - \beta d \tag{10}$$

where α is a scaling factor and β describes the timescale at which the dust settles out of the atmosphere.

This equation was altered to reflect the relationship of dust uplift to wind speeds, as described in section 1.5. This section concluded that some of the uplift was proportional to the wind speed squared, and some was proportional to the wind speed cubed. Thus it could be considered that

$$\dot{d} = \alpha(f^2 + s^3) - \beta d \tag{11}$$

is also a suitable dust uplift model. Comparisons of the two dust profiles can be seen in figure 11. Figure 11a) shows the profile when dust is proportional to u^2 only; 11b) is a plot of the dust when it is proportional to u^3 only. Assuming the amount of dust which is

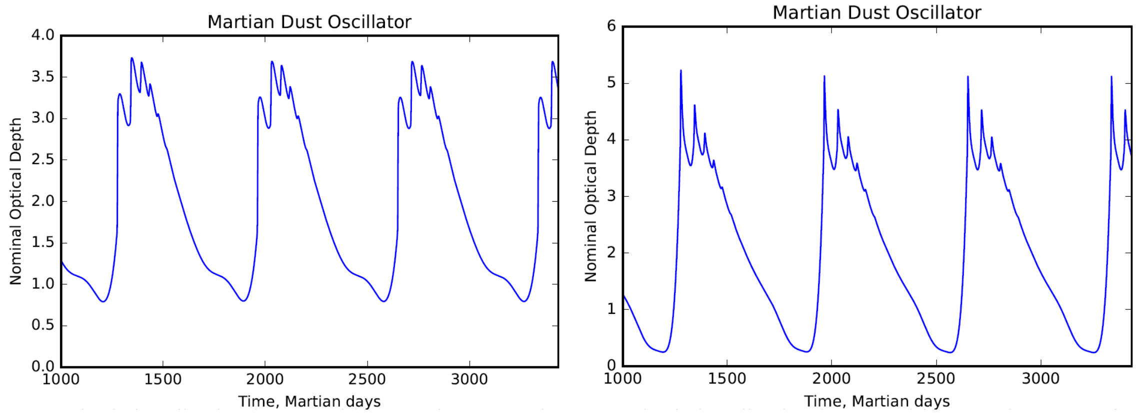

(a) Using equation 10 (b) Using equation 11

Figure 11: Proposed relationships of dust to heat flux. Note the different y-axes.

lifted by mean winds (u^3) and by dust devils (u^2) is of similar magnitude, and assuming that s is of order 1, the dust equation was chosen to be:

$$\dot{d} = \alpha(f^2 + 0.5s^2 + 0.5s^3) - \beta d \tag{12}$$

Figure 12 shows the profile of the dust when it scales in the form of equation 12. For the purposes of this project, α is set to be equal to 0.005, and β is set as 0.03. This ensures that the dust content does not grow larger year upon year, while also preventing it from reducing completely to zero, as the Martian atmosphere always has suspended in it a low level of dust. α is set as a low value simply to scale the dust levels, and keep all the variables to similar orders of magnitude.

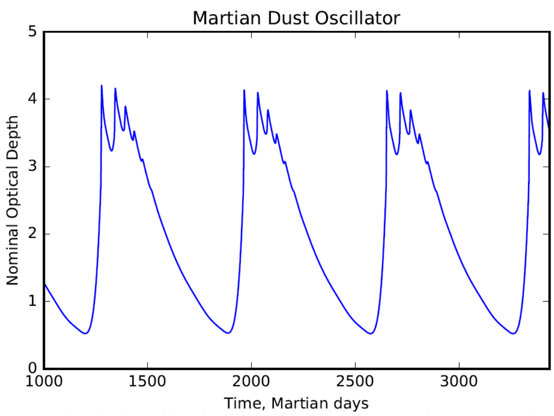

Figure 12: Relationship of dust to heat flux, using equation 12

Figure 13 shows a run of the model including passive dust. The relationships can be seen easily, and the system is very regular and periodic, as expected. The dust loading does not vary from year to year, and includes several peaks that correspond to the dust content's relationship with the baroclinicity.

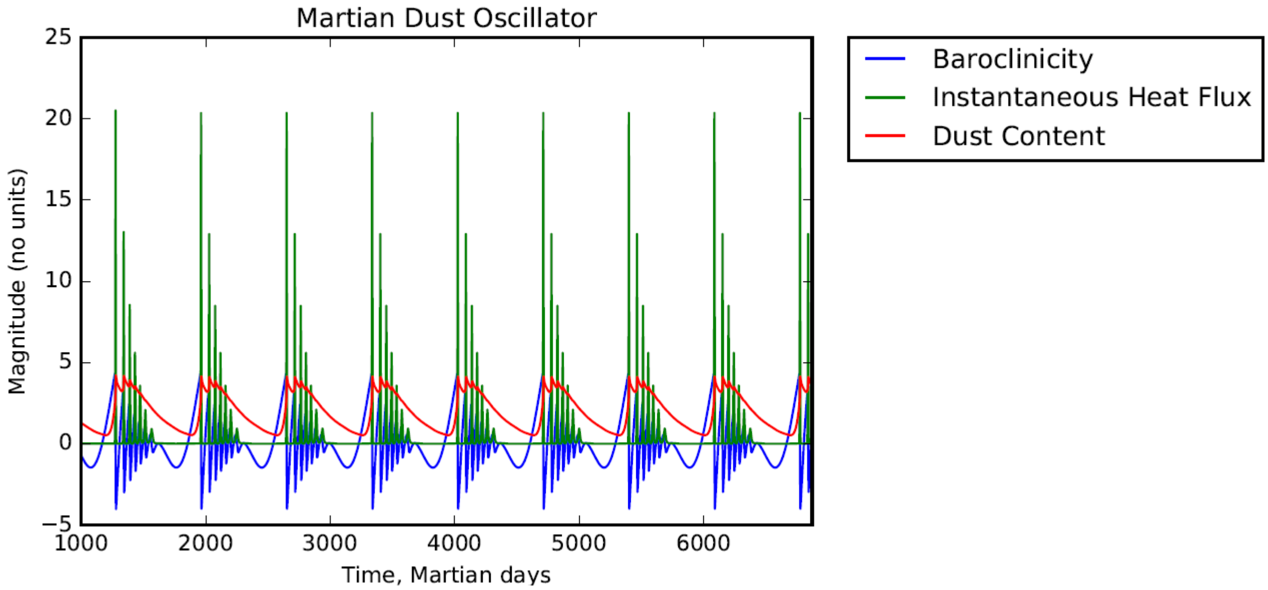

Figure 13: Passive dust, showing the relationships of all variables, using equation 12. This is the same model run as in figure 12, but showing traces of all variables, rather than only the dust.

This system does not capture the non-linear feedback mechanisms of the third parameter. In effect, it describes how radiatively inert dust would react to the Ambaum-Novak equations. To make the system more realistic, the radiative nature of the dust needs to affect the heat flux and baroclinicty: ie. 'active' dust needs to be added.

3.2 ACTIVE DUST

We know that dust lifted into the atmosphere is heated by solar insolation and therefore heats the air around it. Thus, when dust is lifted by a baroclinic storm or dust devil, it has a destabilising effect, either by enhancing the storm or deepening the convection. Enhancing the winds in a baroclinic storm will cause more dust uplift, and similarly deepening convection in a dust devil will strengthen the vortical suction, which causes more dust to be lifted.

However, this effect only occurs at low dust concentrations. At high dust concentrations, such as those during a global dust storm, the sun can only reach the higher levels of the dust before it is absorbed. Thus, the higher levels of the atmosphere are heated more quickly than the surface, and a temperature inversion occurs. This temperature inversion causes the surface winds to die down and convection to cease, so the dust which initially had a destabilising effect at lower concentrations eventually causes stabilisation of the atmosphere at very high concentrations. Also, the baroclinic growth rate is inversely proportional to the vertical stability, so at high dust concentrations, this forces the baroclinic growth rate to reduce.

To capture this, the equation for heat flux was reformulated to include a term which reflected the radiative effect of the dust. Initially, the stabilising and destabilising effects were considered separately:

$$\dot{f} = 2sf(1 + \gamma d) \tag{13}$$

which represents a linear upward slope, and describes the dust enhancing the growth rate of the eddies, and:

$$\dot{f} = \frac{2sf}{(1 + \zeta d)} \tag{14}$$

which represents a downward slope, which tails off to zero, and captures the stabilising and damping effects of the dust.

It is interesting to compare the stabilising and destabilising dust profiles, as shown in figure 14. It can be seen in figure 14a) that the destabilising effect produces a very strong, periodic feedback, whereas in figure 14b), the stabilising function produces an effect with a period of 3 Martian years, which much lower peaks in the heat flux.

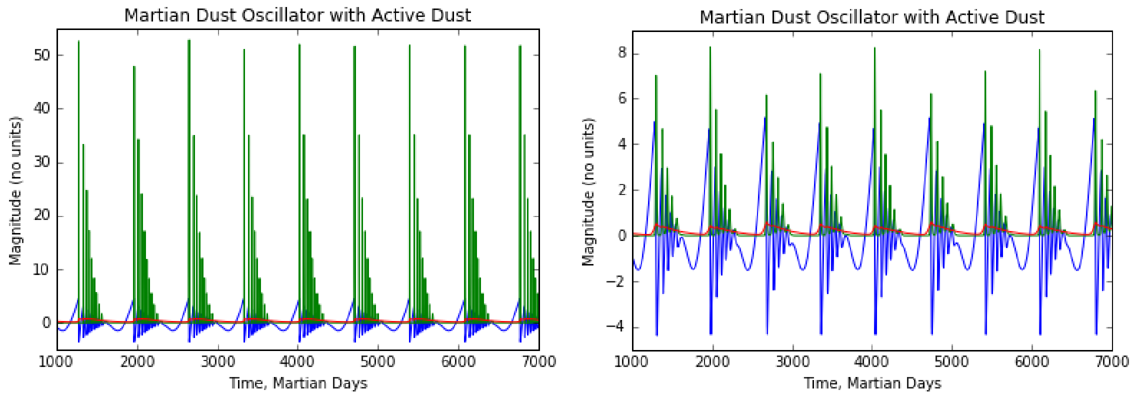

(a) Using equation 13 (b) Using equation 14

Figure 14: Active dust runs comparing the stabilising and destabilising effects of the dust. Blue trace is the baroclinicity, green lines represent the instantaneous heat flux and the red trace is the atmospheric dust content.

Combining equations 13 and 14, it was suggested that

$$\dot{f} = \frac{2sf(1+\gamma d)}{(1+\zeta d^2)} \tag{15}$$

may be a realistic distribution, where γ and ζ are constants. γ represents the factor determining the strength of the amplification, and ζ determines the strength of the damping. Figure 15(a) shows the shape of this function. At zero dust, it means that the original Ambaum-Novak equations are recovered, which is important. It then acts to enhance the storms at low levels, but reduces the wind speeds at higher levels, as the function tails off. Another profile for the dust was suggested, which had a sharper reduction to zero, describing a more sudden stabilisation by high dust levels:

$$\dot{f} = 2sf(1+\gamma d)e^{-\zeta d^2} \tag{16}$$

The profile of this equation is shown in figure 15(b).

Featured in figure 16 is the time series plot for the function in equation 16. It was found that this function was only stable for certain values of γ and ζ, and that the most

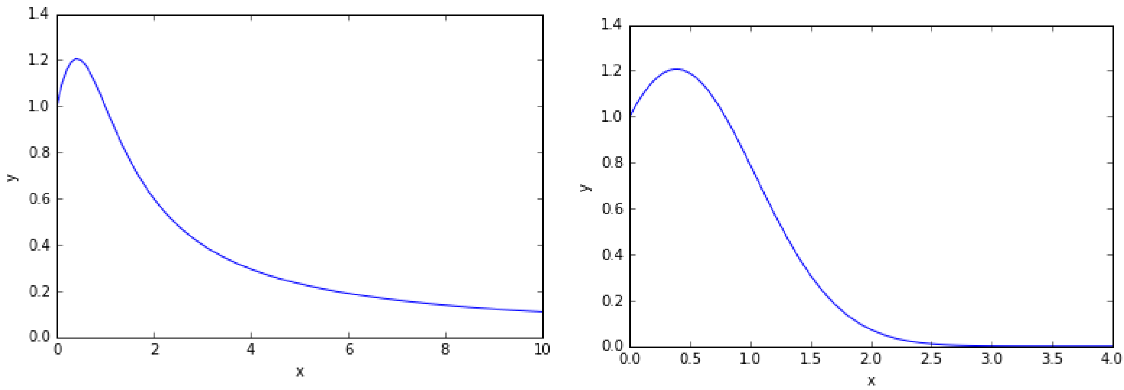

(a) $y = \frac{(1+x)}{(1+x^2)}$ (b) $y = (1+x)e^{-x^2}$

Figure 15: Proposed functions for active dust. Note the different scales on the x-axis.

interesting behaviour was exhibited for the highest stable value of ζ - ie. a very large damping effect. In figure 16, ζ = 0.93 and γ = 1.

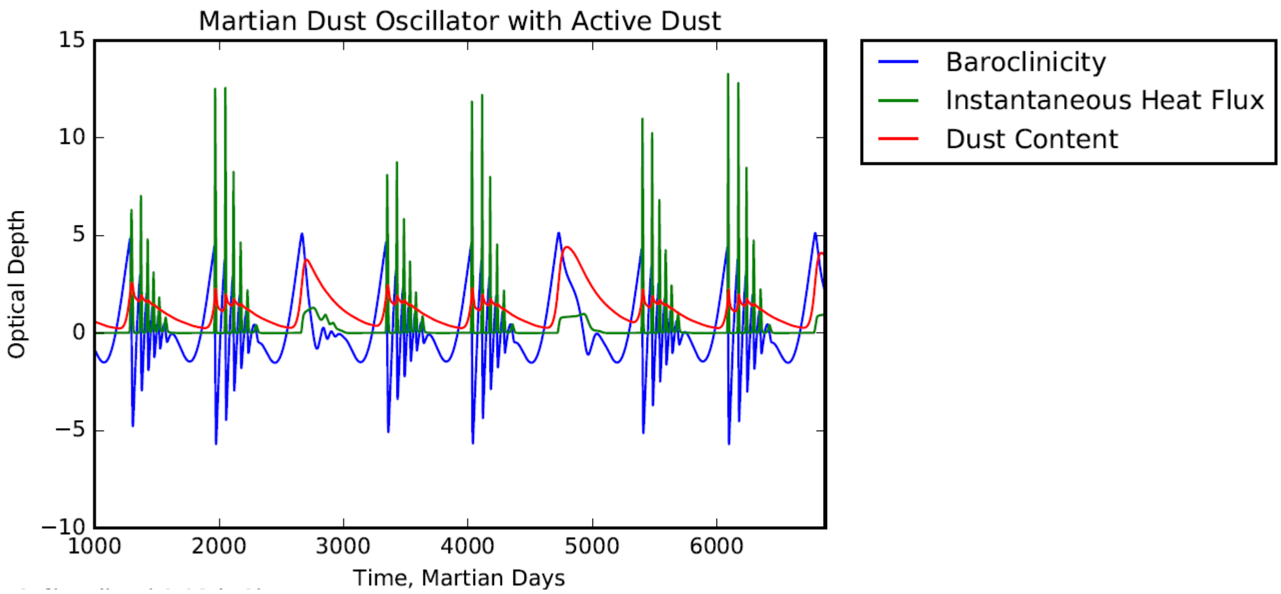

Figure 16: A time series using the dust relationship in equation 16, which appears to have a 4-year cycle, but in fact the cycle has different peaks and behaviour each time.

It is already clear that this shows more interesting behaviour than the passive dust runs shown in figure 13. There are still peaks every year, but they are not of the same height, and peaks show different shapes. It is not clear from this short run whether there is any periodicity - this must be determined by plotting a much longer run in phase space. Figure 17 shows the phase space plot for the same parameters as figure 16.

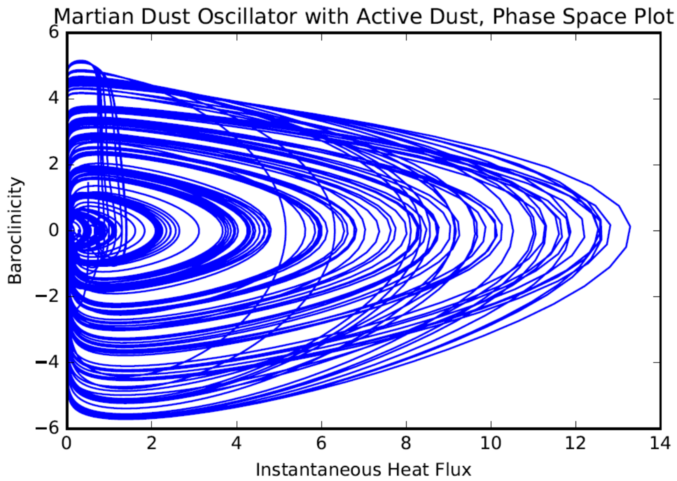

Figure 17: A phase space plot using the dust relationship in equation 16, which appears to have little repetition and regularity.

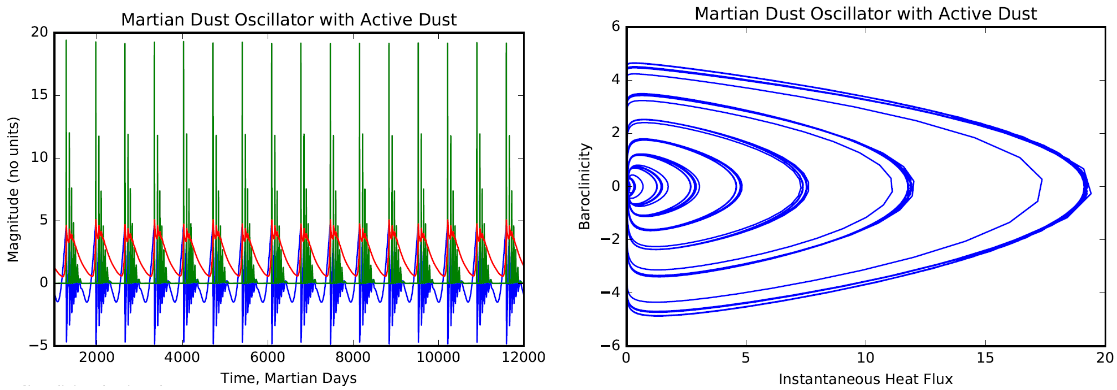

(a) Time series (b) Phase space plot

Figure 18: Active dust run using equation 15, with $\gamma = \zeta = 1$

It can be seen in the phase space plot using equation 16, that there is little repetition or periodicity. The relationship between the baroclinicity and the instantaneous heat flux may be considered to be chaotic for this radiative dust profile, but this function is more fragile, so it is difficult to investigate this behaviour further.

Equation 15 appears to be less fragile, and stable for more values of γ and ζ. Hence it is interesting to investigate how changing these values, and hence changing the relative importance of the destabilising and damping effects, changes the system. In figure 18, a time series and phase space plot of the system when $\gamma = \zeta = 1$ is shown.

In figure 19, several plots are shown, with γ remaining at 0.8, while ζ is altered. Changing ζ alters the system strongly, with different values of ζ changing the periodicity of the system.

Each figure displays behaviour typical to the system: low dust years feature many storms in the winter season; high dust years suppress eddy activity and cause larger fluctuations in the range of the baroclinicity. Every year, the instability builds over the summer season, causing a sharp increase in eddy activity during the winter season in low dust years. In high dust years, this buildup of instability causes the atmospheric dust content to rise sharply in the winter.

From the figures, it can be seen that changing ζ has a strong effect on the system, and it appears that very small and very large values of ζ produce more periodic results. However, it can be seen in figure 19g), that very high damping values cause the system to be 'kicked' into a different regime, in which the heat flux is damped too heavily and reduces to zero, causing the atmospheric dust content to depend on the baroclinicity only. This causes larger spikes in the dust content lasting for several years, and though from observations, we know this is an unrealistic scenario, the behaviour of the model at high damping levels is interesting to observe.

The phase space diagram in figure 19d) is particularly interesting, as it appears to display fully aperiodic behaviour. Further study may include more tests of parameters near these values of γ = 0.8 and ζ = 5.

Figure 20 shows a number of runs where ζ remains constant at 5, and γ is altered.

The unrealistic behaviour exhibited in figure 19g) can also be seen in figure 20a), showing that low values of γ can also cause the system to move into the another regime. The systems which reach this other regime seem to also have a higher level of periodicity. The other runs of this experiment seem to show high levels of aperiodicity, which again suggests that values around ζ = 5 may exhibit the chaotic behaviour this report is seeking.

In section 3.1, it was determined that $\dot{d} = \alpha(f^2 + 0.5s^2 + 0.5s^3) - \beta d$ was a suitable function for the dust relationship. The runs in figures 19 and 20 have all used this dust uplift model. However, it is worth investigating how the system reacts to different

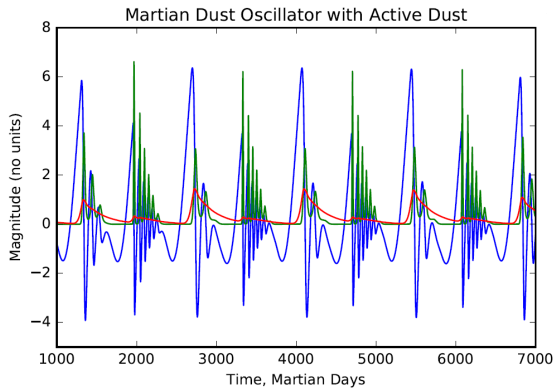

(a) Time series, $\zeta = 4$

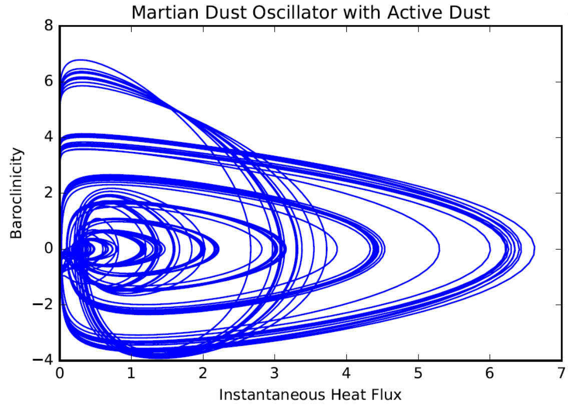

(b) Phase space, $\zeta = 4$

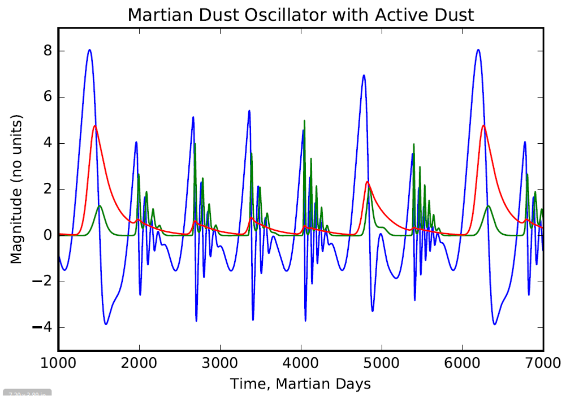

(c) Time series, $\zeta = 5$

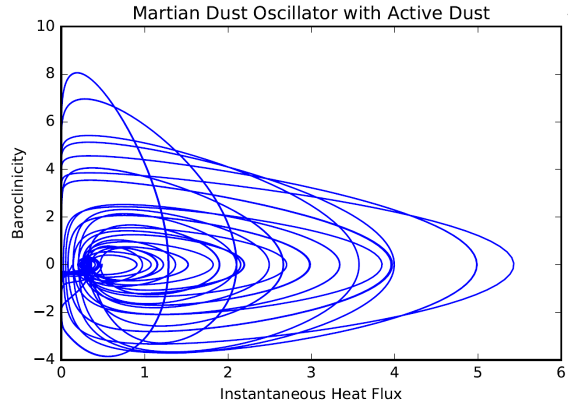

(d) Phase space, $\zeta = 5$

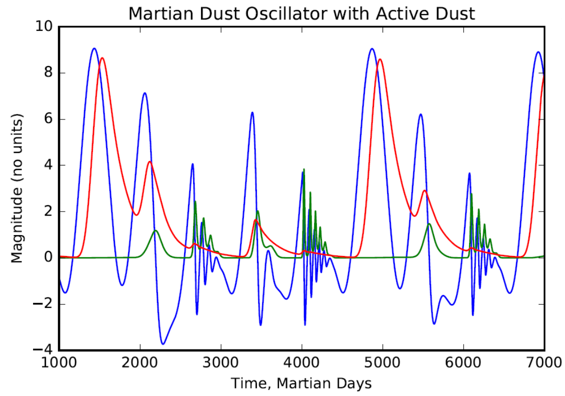

(e) Time series, $\zeta = 7$

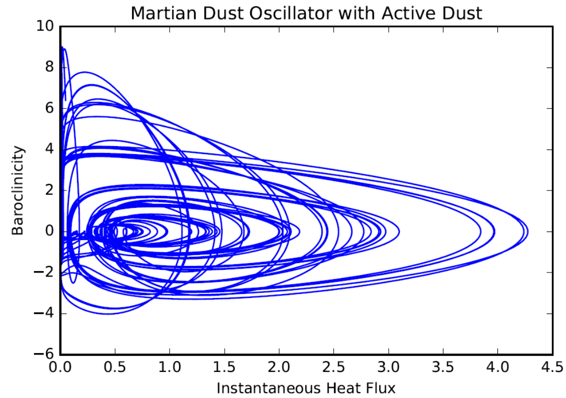

(f) Phase space, $\zeta = 7$

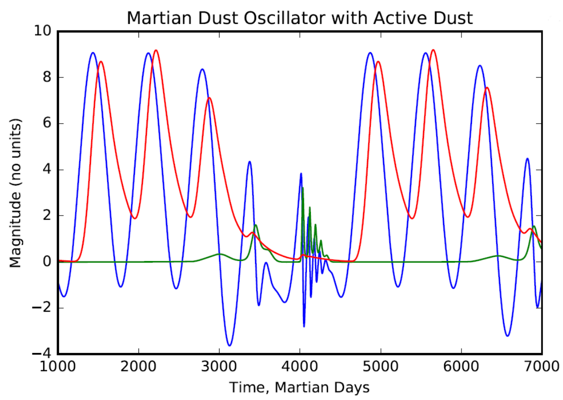

(g) Time series, $\zeta = 10$

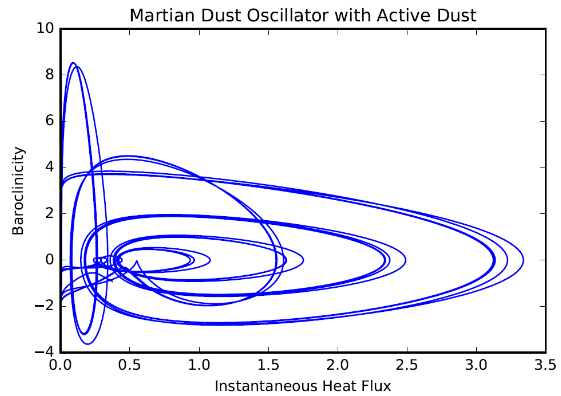

(h) Phase space, $\zeta = 10$

Figure 19: Time series and phase space plots, all with $\gamma = 0.8$. For all plots on the left, blue lines are the baroclinicity, green lines represent the instantaneous heat flux and the red trace is the atmospheric dust content.

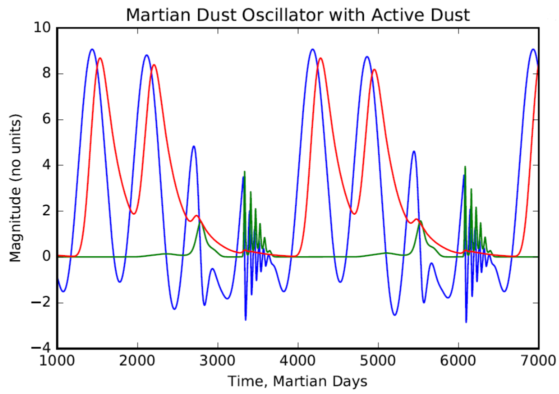

(a) Time series, $\gamma = 0.4$

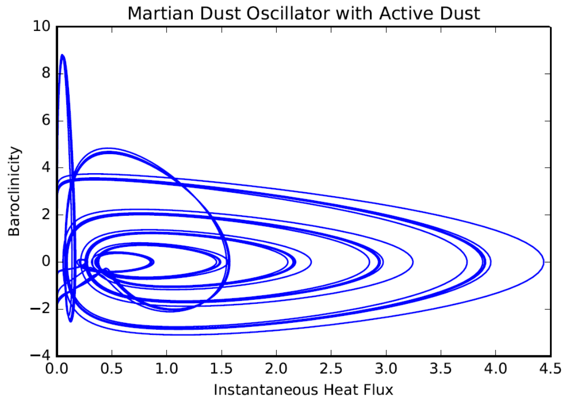

(b) Phase space, $\gamma = 0.4$

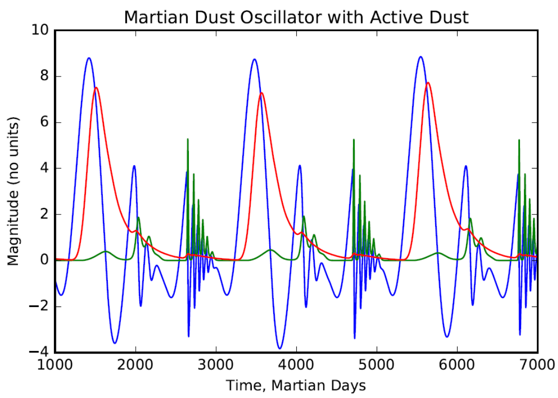

(c) Time series, $\gamma = 0.7$

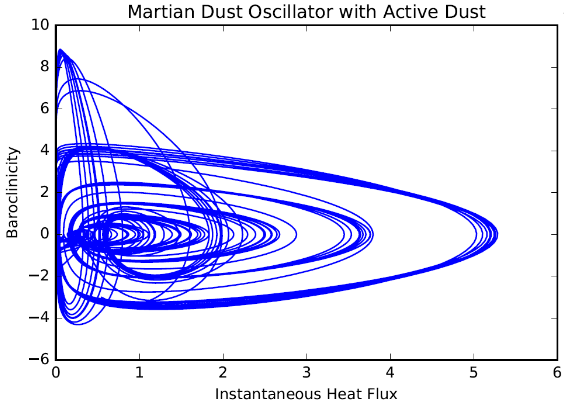

(d) Phase space, $\gamma = 0.7$

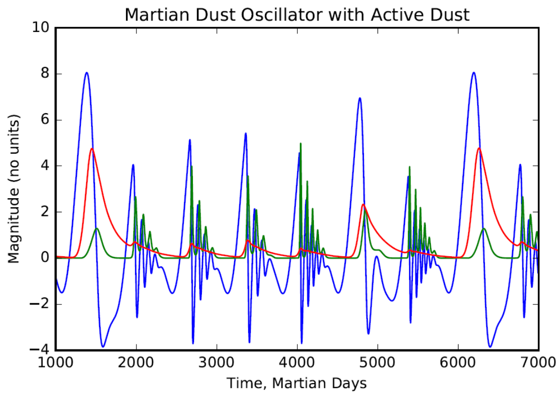

(e) Time series, $\gamma = 0.8$

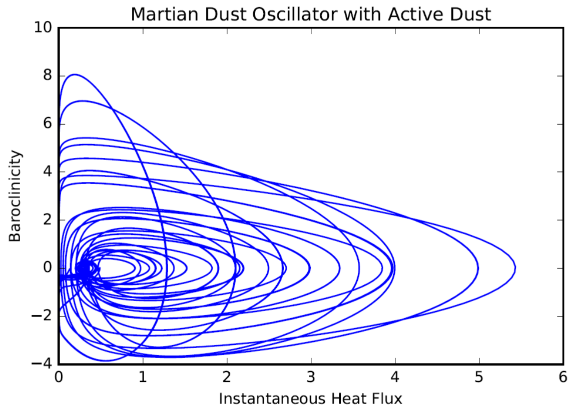

(f) Phase space, $\gamma = 0.8$

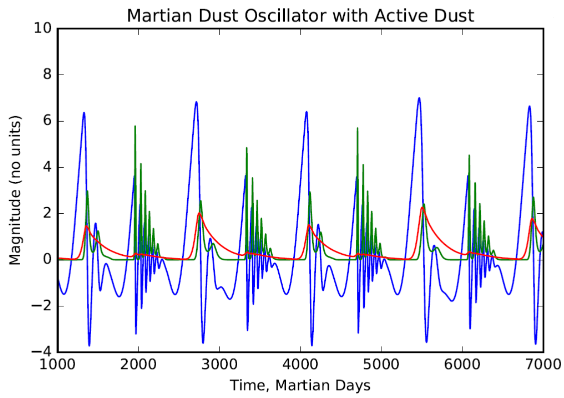

(g) Time series, $\gamma = 1.0$

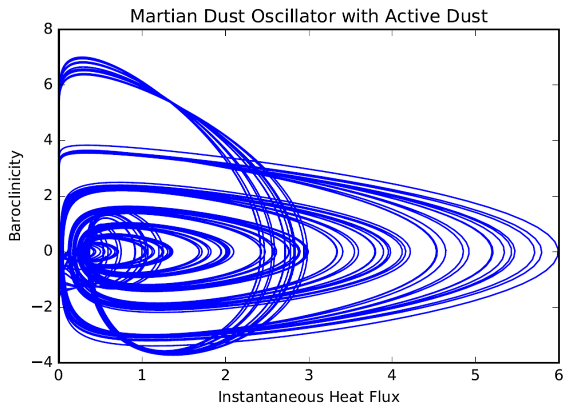

(h) Phase space, $\gamma = 1.0$

Figure 20: Time series and phase space plots, all with $\zeta = 5$. For all plots on the left, blue is the baroclinicity, green lines represent the instantaneous heat flux and the red trace is the atmospheric dust content.

proportions of s^2 and s^3, using $\dot{d} = \alpha(f^2 + as^2 + (1-a)s^3) - \beta d$, which corresponds to the atmospheric dust content being either more heavily influenced by dust devils, or by the mean winds, with a ranging from 0 to 1. All of the runs in figure 21 use $\zeta = 5$ and $\gamma = 0.8$.

As can be seen in figure 21, runs where all or most of the dust uplift is caused by dust devils (where a is high, and s^2 dominates the uplift) display strong periodicity. They also have much smaller amplitudes. As a grows smaller, and s^3 comes to dominate the uplift, which corresponds to the dust being mainly lifted by the mean winds, the amplitudes grow, and the peaks begin to become less predictable. When $a = 0$, and there is no influence from dust devils, the huge peaks appear in subsequent years, which we know is not realistic behaviour for Martian dust storms. When a is small, this aperiodic behaviour is also shown, but the peaks are solitary, which is behaviour we do see in the Martian atmosphere. This experiment shows that the influence of the s^3 from the mean winds may be a more important factor for causing the interannual variability to take on chaotic behaviour.

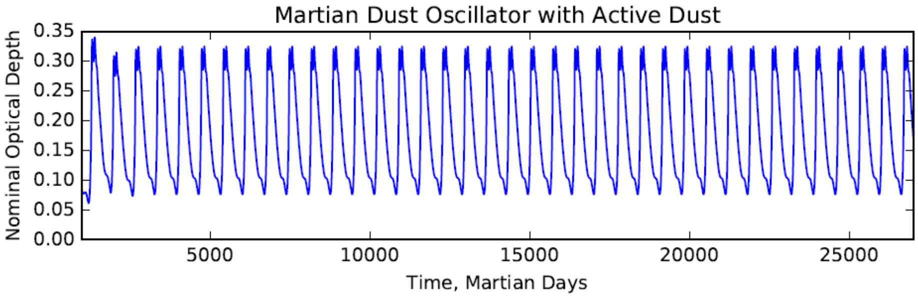

(a) $a = 1$, ie. no s^3 influence

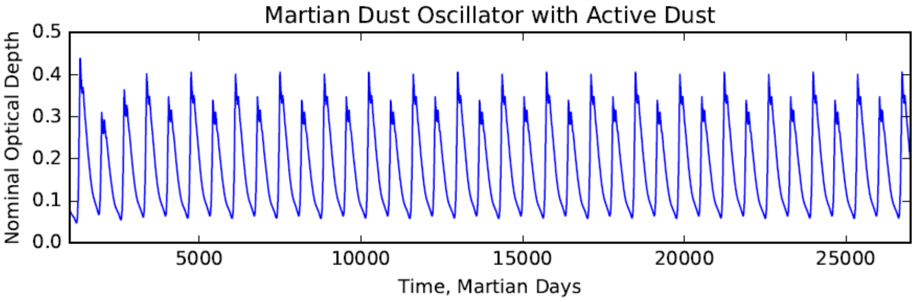

(b) $a = 0.8$

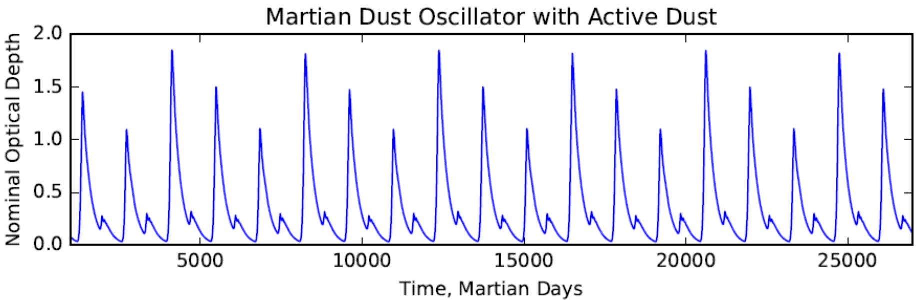

(c) $a = 0.6$

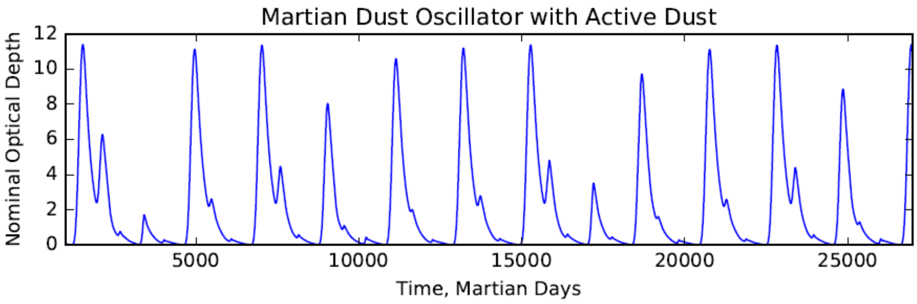

(d) $a = 0.3$

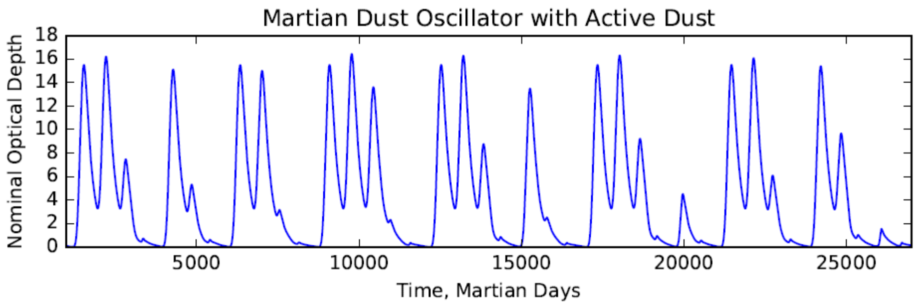

(e) $a = 0$, ie. no s^3 influence

Figure 21: Active dust runs, using different values corresponding to stronger influences of either dust devils or mean winds. In order of decreasing a, corresponding to decreasing importance of dust devils.

4

SUMMARY AND CONCLUSIONS

Martian dust storms occur globally, but do not occur at predictable intervals. This dissertation aimed to determine whether this is due to the inherent chaotic nature of Mars' interannual variability, arising from the coupling between the dust and baroclinic storms.

Dust uplift on Mars is dependent on a number of factors, but it seems to be the main source of the interannual variability, so it is important to be able to estimate this accurately, and to determine how the relative influence of dust devils and mean winds for uplift affects the circulation and dust content.

Experiments suggest that a dust profile which has nearly equal influences from the wind speed squared and the wind speed cubed, which corresponds to the uplift from dust devils and mean winds respectively, shows realistic behaviour. However, systems which have a slightly stronger influence from u^3 tend to show behaviour which is more aperiodic.

The low order model developed during the course of this project has shown to be versatile and displays some of the behaviour that has been observed in the Martian atmosphere. When the dust is passive, and not allowed to interact, radiatively or otherwise, with the other variables in the Ambaum and Novak equations, the dust increases each winter season, and then reduces to a low value at the end of the summer. The peaks are the same height every year, and the system shows no interannual variability, which is expected.

Two models for the radiative effects of active dust were tested, where the dust is allowed to destabilise the atmosphere at low concentrations, and display damping behaviour at high concentrations. Two profiles were considered: the first, $\dot{f} = 2sf(1+\gamma d)e^{-\zeta d^2}$ showed chaotic behaviour for high damping values, but was also very fragile and the parameters could not be changed very much before the system was kicked into an unrealistic state, where the heat flux reduces to zero and does not recover. Thus, while this system shows interesting behaviour, it does not display the flexibility of the other radiation model.

The other radiation model, $\dot{f} = \frac{2sf(1+\gamma d)}{(1+\zeta d^2)}$ does not show damping behaviour that is as strong as the other function at high dust levels. Because of this, γ and ζ were able to be altered across a large range of values. Many of these values caused the system to show periodic behaviour, either on a 1 year cycle, or several years. Many of the versions of this system, however, showed highly aperiodic behaviour, either displaying a periodic cycle that was very long, or truly chaotic patterns.

It is not known whether the dust storms on Mars follow a truly chaotic pattern, or whether it is simply a complicated multi-year cycle. This is due to a lack of observations: there have been a few hundered years of telescope observations of the planet, but these are intermittent and can be unreliable. Satellites and surface landers have only been on the planet for a few decades, and no surface measurements have been made consistently for more than a few years at a time.

It is possible to determine whether a system is chaotic by analysis of the phase space diagrams by sight. A periodic system will have lines which cross over or follow the same paths. A chaotic system must never have intersecting lines in 3-D phase space, as the system does not self-repeat by definition. Further research, however, may include determining the chaotic nature of the system mathematically, by calculating its Lyapunov exponents. Every system has associated with it a set of Lyapunov exponents, and as long as the system is globally stable, if the value of the largest Lyapunov exponent is positive, it can be considered that the system is chaotic.

Further runs of the existing model would include factors around γ = 0.8 and ζ = 5, which seemed to show very interesting, chaotic behaviour. Perhaps experiments near these values could also be made using a stronger influence of dust uplift due to the mean winds, which is proportional to u^3, which was shown to produce more aperiodic behaviour.

It has been suggested in the literature that the interannual variability may depend on dust availability from year to year. When a great deal of dust is available to be lifted, it may cause a large dust storm, but if this redistributes the dust to areas where it is less likely to be lifted into the atmosphere, the following year is likely to be clear. This could be achieved using the low order model by splitting the dust variable into two equations: one describing the dust content of the northern hemisphere and one for the southern hemisphere, where the southern hemisphere acts as a reservoir for dust.

Of course, there are many models which feature more complex aspects of the Martian dust cycle. As well as hemispheric reservoirs, a model could consider deposits of sub-tropical and polar dust, or include the aspect of dust deposition into the polar caps as condensation nuclei for carbon dioxide snow. Ingersoll and Lyons (1993) considered upper and lower level dust separately. A number of Mars GCMs have been developed in recent decades, which capture all aspects of the Martian circulation and climate. Newman et al. (2002a, 2002b) developed a full Mars dust uplift model for the Oxford Mars GCM.

It is, however, the simple nature of this low order model which we find interesting to investigate. That chaotic behaviour can arise from the basic interaction between the dust and the baroclinic storms is an attractive result from the simple model. Mars GCMs are limited due to the lack of observations of Mars compared to Earth, and require a great deal of computing power, so therefore our model provides an attractive alternative of extreme simplicity.

5

REFERENCES

Ambaum, M. H. P., and Novak, L., 2014: A nonlinear oscillator describing storm track variability. *Q. J. R. Meteorol. Soc.* **140**: 26802684, doi:10.1002/qj.2352

Barnes, J. R., 1984: Linear Baroclinic Instability in the Martian Atmosphere. *J. Atmos. Sci.* **41,9**: 1536-1550

Blumsack, S. L., and Gierasch, P. J., 1972: Mars: The Effects of Topography on Baroclinic Instability. *J. Atmos. Sci.* **29**: 1081-1089

Collins, M. et al., 1996: Baroclinic Wave Transitions in the Martian Atmosphere. *Icarus* **120**: 344357

Fuerstenau, S. D., 2006: Solar heating of suspended particles and the dynamics of Martian dust devils. *Geophys. Res. Lett.* **33, L19S03**: doi:10.1029/2006GL026798

Gierasch, P. J., and Goody, R. M., 1972: Effect of Dust on the Temperature of the Martian Atmosphere. *J. Atmos. Sci.* **29**: 400-402

Gierasch, P. J., 2002: The north-south martian divide. *Nature* **416**: 269-270

Greeley, R., and Iversen, J. D., 1985: *Wind as a Geological Process on Earth, Mars, Venus and Titan.* Cambridge Planetary Science Series no. 4., 333 pp.

Haberle, R. M., 2003: Mars, *Planetary Atmospheres*, Beatty, J. K., Elsevier Science Ltd., 1745-1755

Hess, S. L., 1950: Some Aspects of the Meteorology of Mars. *J. Atmos. Sci* **7,1**: 1-13

Hollingsworth, J. L., and Barnes, J. R., 1995: Forced Stationary Planetary Waves in Mars' Winter Atmosphere. *J. Atmos. Sci.* **53,3**: 428-448

Hollingsworth, J. L., et al., 1996: Orographic control of storm zones on Mars. *Nature* **380**: 413-416

Ingersoll, A. P., and Lyons, J. R., 1993: Mars Dust Storms: Interannual Variability and Chaos. *J. Geophys. Res.* **98,E6**: 10951-10961

Kuroda, T., et al., 2007: Seasonal changes of the baroclinic wave activity in the northern hemisphere of Mars simulated with a GCM. *Geophys. Res. Lett.* **34,L09203**: doi:10.1029/2006GL028816

Lorenz, E., 1963: Deterministic Nonperiodic Flow. *J. Atmos. Sci.* **20**: 130-141

Michelangeli, D. V. et al., 1987: Barotropic Instability of Midlatitude Zonal Jets on Mars, Earth and Venus. *J. Atmos. Sci.* **44,15**: 2031-2041

Newman, C. E., et al., 2002a: Modeling the Martian dust cycle 1. Representations of dust transport processes. *J. Geophys. Res.* **107,E12**: 5123, doi:10.1029/2002JE001910

Newman, C. E., et al., 2002b: Modeling the Martian dust cycle 2. Multiannual radiatively active dust transport simulations. *J. Geophys. Res.* **107,E12**: 5124, doi:10.1029/2002JE001920

Newman, C. E. et al., 2004: Investigating atmospheric predictability on Mars using breeding vectors in a general-circulation model. *Q. J. R. Meteorol. Soc.* **130**: 29712989, doi: 10.1256/qj.03.209

Read, P. L. et al., 1998: Wave Interactions and Baroclinic Chaos: A Paradigm for Long Timescale Variability in Planetary Atmospheres. *Chaos, Solitons Fractals* **9,1**: 231-249

Read, P. L., and Lewis, S. R., 2004: *The Martian Climate Revisited, Atmosphere and Environment of a Desert Planet.* Springer-Verlag, 326 pp.

Read, P. L., et al., 2015: The physics of Martian weather and climate: a review. *Rep. Prog. Phys.* **78**: doi:10.1088/0034-4885/78/12/125901

Renno, N. O., et al., 1998: A Simple Thermodynamical Theory for Dust Devils. *J. Atmos. Sci.* **55**: 3244-3252

Sinclair, P. C., 1973: The Lower Structure of Dust Devils. *J. Atmos. Sci.* **30**: 1599-1619

Tanaka, H. L., and Arai, M., 1999: Linear baroclinic instability in the Martian atmosphere: Primitive equation calculations. *Earth Planets Space* **51**: 225232

Verhulst, F., 1985: *Nonlinear Differential Equations and Dynamical Systems.* 2nd ed., Springer-Verlag, 277 pp.